Journal of *Marine Science and Engineering*

MDPI

*Article*

# Distribution of Living Benthic Foraminifera in the Baffin Bay and Nares Strait in the Summer and Fall Periods: Relation with Environmental Parameters

**Calypso Racine [1], Jérôme Bonnin [1,*], Pierre-Antoine Dessandier [2] and Jacques Giraudeau [1]**

[1] Université de Bordeaux, CNRS, UMR 5805 Environnements et Paléoenvironnements Océaniques et Continentaux, 33615 Pessac, France; jacques.giraudeau@u-bordeaux.fr (J.G.)
[2] Université de Brest, CNRS, Ifremer, UMR 6197 Biologie et Ecologie des Ecosystèmes Marins Profonds, 29280 Plouzané, France; pierre.antoine.dessandier@ifremer.fr
* Correspondence: jerome.bonnin@u-bordeaux.fr; Tel.: +33-540008857

**Abstract:** Arctic climate warming leads to drastic changes in sea ice dynamics, hence impacting primary productivity but also the benthic communities. Therefore, to assess the response of living benthic foraminifera to contrasting Arctic environments, surface sediments from nine stations were collected during the summer of 2014 and fall of 2015 in the Baffin Bay and Nares Strait. Living standing stock are systematically low in the eastern and western Baffin Bay and much higher in the North Water Polynya and the Kane Basin located at the entrance and in the center of Nares Strait, respectively. High living benthic foraminiferal densities in the NOW reflect higher TOC while the highest density in the Kane Basin coincides with lower TOC but higher C/N and higher $\delta^{13}C_{org}$. The contribution of agglutinated species is on average very high for the whole study area and dominated by the species *Adercotryma glomeratum*, *Lagenammina arenulata*, and *Reophax scorpiurus*. Calcareous species, dominated by *Nonionellina labradorica* and *Melonis barleeanus*, are more abundant in the North Water Polynya and the Kane Basin. The very high living standing stock observed in the Kane Basin might be related to the northern position of the ice arch that summer during 2014 and therefore a particularly scarce sea ice cover might have allowed massive phytoplankton production during that season. In this study, the distribution of living benthic foraminifera is discussed according to several environmental parameters such as water masses, phytoplankton productivity, and organic matter fluxes.

**Keywords:** living benthic foraminifera; Arctic; Nares Strait; sea ice



**Citation:** Racine, C.; Bonnin, J.; Dessandier, P.-A.; Giraudeau, J. Distribution of Living Benthic Foraminifera in the Baffin Bay and Nares Strait in the Summer and Fall Periods: Relation with Environmental Parameters. *J. Mar. Sci. Eng.* **2023**, *11*, 2049. https://doi.org/10.3390/jmse11112049

Academic Editor: Petra Heinz

Received: 20 September 2023
Revised: 23 October 2023
Accepted: 24 October 2023
Published: 26 October 2023



## 1. Introduction

Warming of the Arctic regions observed in recent decades impacts physical, biological, and human systems [1–5]. The Baffin Bay, located on the west of Greenland and connected to the Arctic Ocean by the narrow Nares Strait, experiences rapid and continuous environmental changes with a warmer and wetter atmosphere, shortened snow cover periods, and a decreased in Greenland ice sheet and sea ice thickness [6,7]. These environmental changes potentially impact ocean circulation and mixing [8,9]. Ecosystems of the Baffin Bay are therefore strongly dependent on atmospheric and hydrological regimes and sea ice dynamics that are influenced by the contrast between relatively warm Atlantic water and cold Arctic water. These environmental parameters influence the primary productivity at the surface of the water column but also have an impact on the benthic communities.

The distribution of modern benthic foraminifera in the Baffin Bay and the surrounding regions has been investigated by few authors during the last few decades. Early works [10–13] provided some data on the distribution of benthic foraminifera in the sediment and some basic ideas on the ecology of those organisms in the environments of the Baffin Bay and the Canadian Arctic Archipelago. All studies revealed the omnipresence of agglutinated benthic foraminifera in the cold waters of the Canadian Arctic Archipelago and Baffin Bay continental shelves. The nature of the water masses is shown to be the main factor controlling the distribution of benthic foraminifera observed in these studies. This hypothesis was also developed by Hunt and Corliss [14]. More recently, the study of modern (living and dead) benthic foraminifera in the Baffin Bay and Labrador Sea [15,16] showed that the main parameters controlling benthic foraminifera distribution in those environments are processes of carbonate dissolution and the physical characteristics of water masses. However, Schroder-Adams et al. [17] suggest that sea ice exerts a more important control on the distribution of benthic faunas in the Canadian Arctic Archipelago. The abundance of agglutinated benthic foraminifera compared to calcareous species would be linked to the seasonal dynamic of sea ice, accentuating processes of carbonate dissolution in sediments. Calcareous benthic foraminifera appear to be preserved in environments where sea ice cover is permanent. Based on a study of the central Arctic, Wollenburg and Kuhnt [18] showed that the critical environmental parameter influencing the distribution of benthic foraminifera in terms of density, diversity, and foraminiferal associations is episodic food supply derived from seasonal primary productivity which in turn is closely related to sea ice dynamics.

Benthic foraminifera are frequently used as paleoenvironmental proxy in the Baffin Bay and Nares Strait [19–23], but interpretations made from the paleo-records rely on solid knowledge of the benthic foraminifera ecology in those particular environments. The Baffin Bay and adjacent Nares Strait are locations of very active sea ice dynamics with highly contrasted environments between the deep Baffin Bay, the narrow and relatively shallow Nares Strait, and the North Water Polynya (NOW) that connects those two regions. This study therefore aims at better understanding the distribution of living benthic foraminifera in summer and fall periods in those regions in relation to water depth and water masses, sea ice cover, and primary production.

## 2. Environmental Settings

### 2.1. Baffin Bay

The Baffin Bay is a marginal sea of the North Atlantic Ocean surrounded by Baffin Island to the west, Greenland to the east, and Ellesmere Island to the north (Figure 1). This semi-enclosed basin has an average depth of 2400 m [16]. To the west, the shelf is narrow, steep, and cut by several deep trenches. To the east, the shelf is wider and cut by glacial paleovalleys. Sedimentation in the Baffin Bay is mainly controlled by terrigenous detrital inputs owing to debris flows, turbidite events, and ice-rafted material [24,25]. One of the features of the Baffin Bay is the shallow depth of the carbonate compensation depth (CCD). Aksu [26] suggested that the CCD occurs at a depth of between 600 to 900 m and the foraminiferal lysocline may be as shallow as 100–300 m.

The Baffin Bay is connected to the north to the Arctic Ocean through several narrow channels of the Canadian Arctic Archipelago and Nares Strait and to the south to the Atlantic Ocean via the Davis Strait. Ocean circulation is cyclonic and comprises two main currents (Figure 1). To the east of the bay, the West Greenland Current (WGC) transports modified Atlantic water mass that is relatively warm and salty [27]. Several branches of this current carry Atlantic water in the middle of the Baffin Bay. Along the Canadian coast, a colder and less salty Arctic water mass flows southward by the Baffin Current (BC). This ocean circulation affects the dynamic of sea ice [28]. In winter, the bay is entirely covered with sea ice. The sea ice extent is maximal in February and March. From April to August, the sea ice extent decreases progressively reaching a minimum in August and September. The retreat of sea ice occurs from south-east to north-west owing to the presence of a relatively warm water mass coming from the Atlantic Ocean to the north along the Greenland coast.

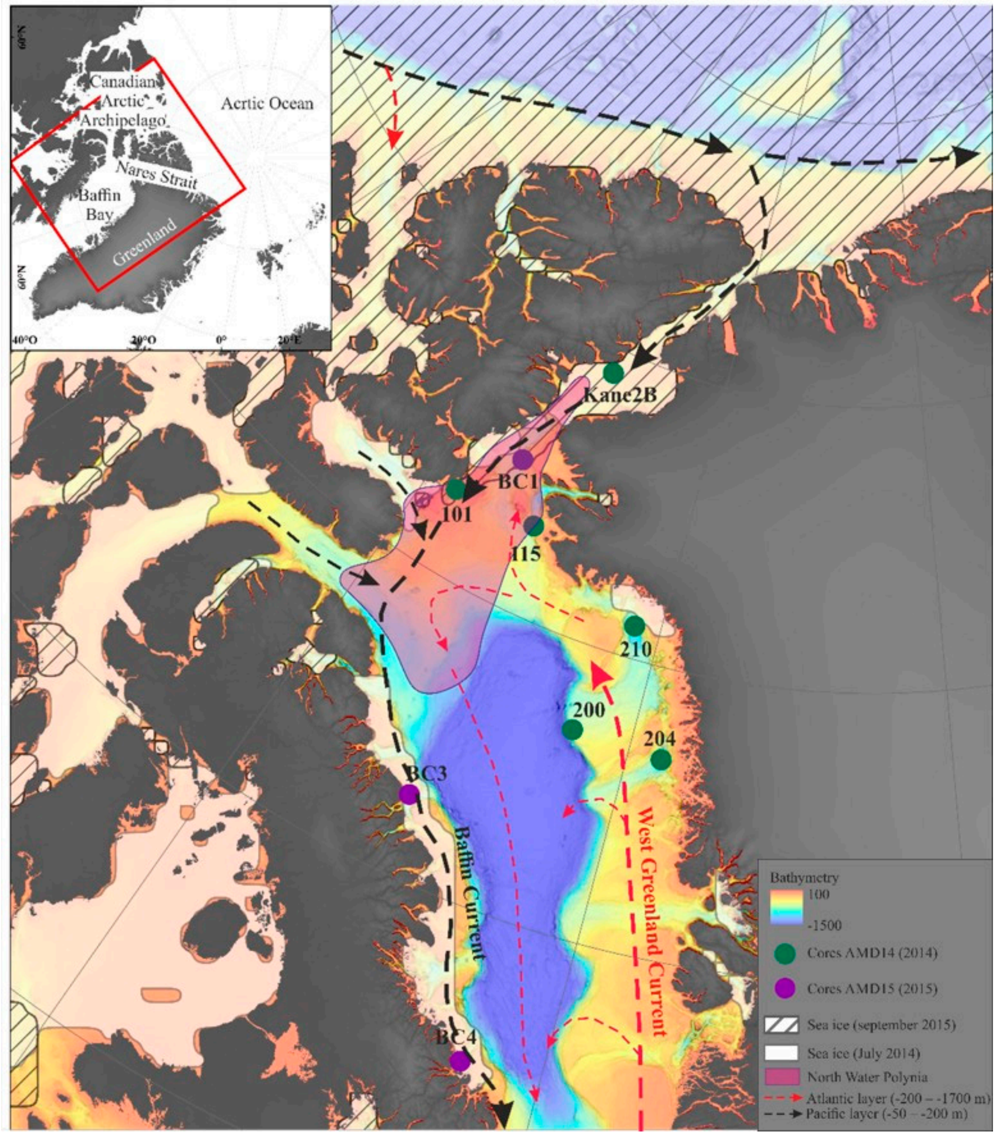


**Figure 1.** Bathymetric map of the Baffin Bay with sampling locations of cores from AMD14 and AMD15 expeditions, sea ice extent in July 2014 (white) and September 2015 (hatched), and circulation of main currents adapted from Solignac et al. [29].

During springtime and summertime, the annual melt of sea ice influences phytoplankton blooms and therefore benthic ecosystems. Intense blooms are observed near the ice edges during the melting period [30,31]. Several factors, such as solar energy, input of fresh water, and nutrients, tend to stimulate primary productivity in these areas. This phytoplankton production constitutes a major supply of food for benthic organisms including benthic foraminifera [32–34]. In the Baffin Bay, annual primary production varies from 60 to 120 gC·m$^{-2}$ [35,36].

*2.2. Nares Strait*

Nares Strait, narrow and 530 km long, separates the north-west of Greenland from Ellesmere Island (Figure 1). It extends from the north of the Baffin Bay to the Lincoln Sea in the Arctic Ocean and constitutes the major connection in the region between the Arctic Ocean and the Atlantic Ocean via the Baffin Bay. Ocean circulation flows to the south from the Arctic Ocean [37,38]. A powerful north wind also affects the region [39–41]. Arctic water carried through Nares Strait is less salty than Atlantic water found in the Baffin Bay. This arctic water is largely composed of nutrient-rich Pacific-origin water and freshwater from rivers and melting ice [39]. Pacific water is twice as rich in nitrogen and phosphorus and seven times richer in silicate than Atlantic water [42]. These features lead to the rise of primary production especially during sea ice melting and so there is a rise of benthic productivity. A part of the Atlantic water mass coming from the Baffin Bay is carried along the Greenland coast and penetrates into Nares Strait until the Kane Basin [39,43,44]. The Kane Basin with an area of 27,000 km$^2$ is relatively large (120 km maximum) and not very deep (220 m). Many icebergs coming from the Humboldt Greenland glacier discharge in the Kane Basin. From September to June, more than 80% of Nares Strait is covered by sea ice [45]. One of the distinctive features of this strait is the presence of ice arches blocking the ice drift to the Baffin Bay, as well as promoting the formation and the preservation of the NOW [44].

### *2.3. North Water Polynya (NOW)*

Between the north of the Baffin Bay and the southern entrance of Nares Strait, the NOW is considered to be the largest and the most productive Arctic polynya (Figure 1). The polynya starts to grow during the months of March and April and reaches its maximal extent in July with a surface area between 80,000 and 90,000 km$^2$ [45–47]. In summer, the NOW is opened on the Baffin Bay and is no longer strictly a polynya. The presence of the NOW is due to the combination of atmospheric and oceanic factors. The formation of ice bridges to the north allows the blockage of ice drift from the north and brakes the strong north winds, letting the area be ice-free [48–50].

The NOW is important for primary productivity and biodiversity. This ice-free area makes it possible to produce premature spring phytoplankton blooms compared to the Baffin Bay region [51]. The high productivity observed in the polynya is due to the combined action of many physical factors such as the penetration of sunlight, an effective mixing of surface waters by the wind, and the supply of nutrient-rich Pacific water [52–54]. Annual primary productivity reaches 150 gC·m$^{-2}$ in the polynya [52,53]. However, the ecosystem of the polynya is subject to a high inter-annual and seasonal variability [55]. Since the last decade, annual productivity in the polynya has declined significantly [56]. A study by Bergeron and Tremblay [57] showed a reduction of 65% of the net biological productivity between 1997 and 2011 which was attributed to the freshening and increased stratification of surface waters. The extent of the phytoplankton bloom would also have decreased in 10 years [51]. According to Blais et al. [58], this drop of the phytoplankton productivity and the abundance of diatoms is due to changes in sea ice dynamics and the stratification of the water column.

## 3. Materials and Methods

This study is based on interface sediment cores, collected during two oceanographic cruises as part of the ArcticNET program and the ANR GreenEdge project on board the Canadian research vessel NGCC Amundsen (Table 1; Figure 1). The first oceanographic expedition, AMD14, led to the acquisition of five cores at five different stations between 27 July and 4 August 2014. Three other cores were sampled during the cruise AMD15 from 1 October to 1 November 2015.

Sediment was collected from boxcores that were subsampled using push cores of 9 cm in diameter during the AMD14 cruise and 15 cm in diameter during the AMD15 cruise. Upon recovery, sediment cores were sliced from the surface down to 5 cm, every 1 cm for the cores from the AMD14 cruise and every 0.5 cm for the ones of the AMD15 cruise. For each station, one sediment core was used for benthic foraminiferal analysis and another one for sedimentological and geochemical analyses. Temperature and salinity profiles over the whole water column were measured at each station using a conductivity temperature depth (CTD) profiler.

**Table 1.** Station numbers, types, locations, and water depths.

| Cruise | Station | Longitude | Latitude | Water Depth (m) |
|---|---|---|---|---|
| AMD14 | 200 | −63.65 | 73.51 | 1448 |
| AMD14 | 204 | −57.96 | 73.43 | 995 |
| AMD14 | 210 | −61.84 | 75.56 | 1152 |
| AMD14 | 101 | −77.69 | 76.43 | 365 |
| AMD14 | 115 | −71.31 | 76.54 | 655 |
| AMD14 | Kane2B | −70.96 | 79.56 | 217 |
| AMD15 | BC1 | −74.47 | 77.47 | 702 |
| AMD15 | BC3 | −70.90 | 71.40 | 832 |
| AMD15 | BC4 | −63.66 | 67.49 | 689 |

### 3.1. Satellite Data

The phytoplankton biomass distribution range in the study area during the sampling periods is illustrated with average monthly chlorophyll a concentrations (Chl a in mg·m$^{-3}$) in July 2014 and September 2015, derived from satellite data collected by the spectroradiometer MODIS installed on the Aqua satellite. Composite images have a resolution of 4 km and come from NASA's application "Giovanni" [59].

### 3.2. Sedimentological and Geochemical Analyses

For each station, one core was dedicated to sedimentological and geochemical analyses. Between 0.5 and 100 mg of dry sediment was used, depending on the sample and the type of analysis.

Grain size analysis was performed at Environnements et Paléoenvironnements Océaniques et Continentaux (EPOC, Bordeaux, France) using a laser diffraction particle size analyzer (Malvern Mastersizer 2000 hydro G, Palaiseau, France). The analytical error was on average ± 0.02 µm. Grain size was measured on freeze-dried sediment for each core every centimeter from the surface down to 5 cm.

Freeze-dried samples were also used for measuring different geochemical parameters at EPOC. Sedimentary total carbon (TC) and total organic carbon (TOC) contents were measured by dry combustion in a LECO CS-125 carbon analyzer (LECO Corporation, St Joseph, MI, USA) [60]. The total nitrogen (TN) content as well as stable carbon isotope ratios of the organic fraction ($\delta^{13}C_{org}$) and stable nitrogen isotope ratios ($\delta^{15}N$) were determined by an elemental analyzer isotope ratio mass spectrometer (EA-IRMS, ThermoFisher Flash 2000 + Isoprime, Thermo Fisher Scientific, Dreieich, Germany). TOC and $\delta^{13}C_{org}$ were analyzed on carbonate-free sediment after HCl (10%) treatment. The isotopic ratios were reported using the conventional δ notation in per mil (‰) and calibrated according to the international references (standards), with these being V-PDB for $\delta^{13}C_{org}$ values and atmospheric nitrogen (AIR) for $\delta^{15}N$ values [61]. TOC and TN contents are expressed as a percentage of weight of sediment (wt.%). The analytical errors were on average ± 0.1 wt.% for TN and TOC contents and ±0.1‰ for $\delta^{13}C_{org}$ and $\delta^{15}N$. The C/N ratio was calculated by dividing TOC by TN.

### 3.3. Living (Stained) Benthic Foraminiferal Analysis

Samples used for living benthic foraminifera analyses were preserved for several months prior to the study in a 1.5 g·L$^{-1}$ solution of Rose Bengal in 96% ethanol in order to stain the endoplasm of benthic foraminifera living at the time of coring [62,63]. At the EPOC laboratory, samples were wet sieved through 63 and 125 µm meshes sieves. Only the >125 µm fraction was considered for this study. For all stations, all stained individuals in the sediment > 125 µm were hand-sorted under wet conditions (ethanol + Milli-Q water) from the surface down to 5 cm. The pink coloration of living faunas is generally clear by transparency through the tests of the organisms. However, this coloration could display differences between species, varying from light pink to dark red or brownish violet [64]. Moreover, the Rose Bengal staining method may also stain the protoplasm of well-preserved dead organisms in deep and anoxic environments [65,66]. Nevertheless, this method shows reliable results and remains the most appropriate method to study living benthic foraminifera [63]. Strict criteria were applied in order to collect only living individuals: only specimens with all of the chambers coloured, except the last one, were considered to be living [67,68] and some non-transparent tests (miliolids and agglutinated taxa) were broken, after identification, to ensure that the protoplasm was stained. Tubular species such as *Saccorhiza ramosa* were often found fragmented but remained recognizable [16]. Each fragment over 1 mm coloured with Rose Bengal was counted as one individual. Otherwise, we considered five coloured fragments as one individual.

We considered species representing at least 5% of the foraminiferal assemblage to be major species. Major species are shown in Figure A1. Faunal densities for each sample were standardized for a sediment volume of 50 $cm^3$. For each sample, a theoretical volume of sediment was calculated based on the core diameter and the slice thickness. Living standing stock represents the total number of living individuals > 125 µm counted per station, normalized for a 100 $cm^2$ sediment area.

## 4. Results

### *4.1. Environmental Settings*

Water masses in the Baffin Bay have two origins, the Arctic Ocean and Atlantic Ocean. Figure 2 shows temperature and salinity profiles measured at each station allowing us to differentiate water masses in the area. In the Kane Basin, cold and low salinity Arctic water mass (<0 °C; <34) dominates. This Arctic water mass reaches 300 m depth to the northern and the western parts of the Baffin Bay but is shallower in the east, affecting the 200 first meters of the water column.

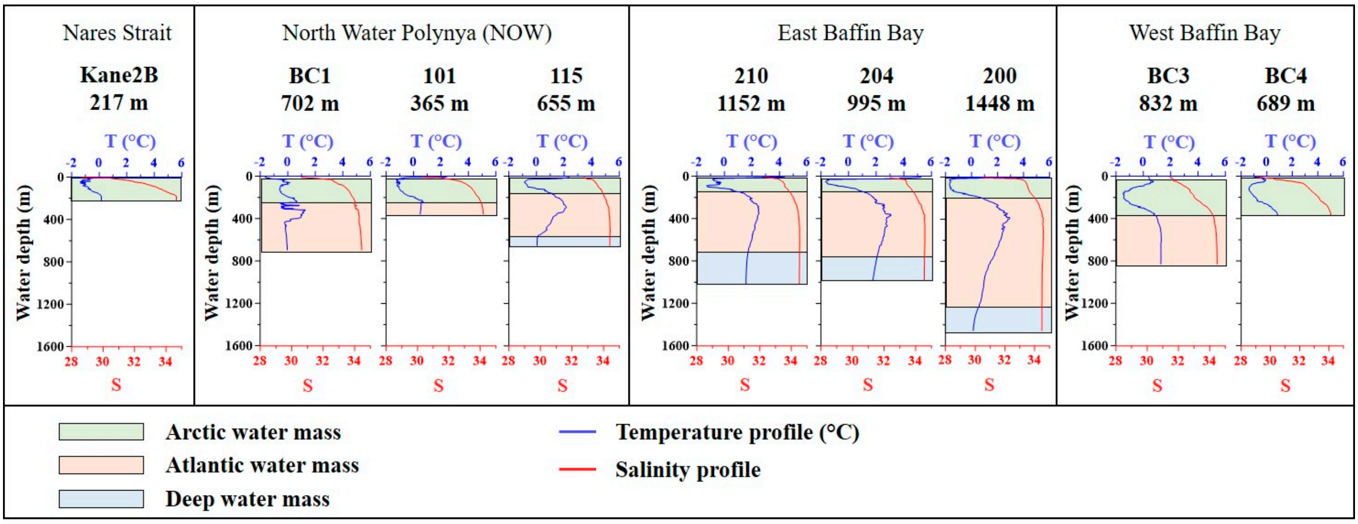


**Figure 2.** Temperature (blue line) and salinity (red line) profiles measured in the water column in July 2014 at stations Kane2B, 101, 115, 210, 204, and 200 and in October 2015 at stations BC1, BC3, and BC4.

The Atlantic water mass is warmer (>0 °C) and saltier (>34). To the eastern part of the Baffin Bay, the WGC transports Atlantic water to the north. The Atlantic water mass occupies a more important volume of the water column in the south than in the northern part of the bay. Indeed, the Atlantic water mass extends to 1200 m water depth at station 200 then becomes progressively less important to the north of the Baffin Bay and reaches 600 m depth at station 115. The temperature of this water mass is higher in the south (around 3 °C) than the north (around 1 °C). Under the Atlantic water mass, there is a colder deep water mass (around 0.5 °C). Salinity is uniform at around 34.5. The differences of the distribution of water masses observed between the stations is reflected in the ocean circulation in the Baffin Bay. Warm and salty water is brought from the Atlantic Ocean along the Greenland coast to the north, and cold and less salty Arctic water is brought from the Canadian Arctic Archipelago and Nares Strait to the south, along the Canadian coast. These results are in line with the observations of [28], which describe the circulation and the distribution of water masses in the Baffin Bay.

Phytoplankton biomass in the studied area mainly gathers to the western and northern parts of the Baffin Bay, in the NOW area, and in Nares Strait (Figure 3). Chl. a concentrations in these areas reach 2 mg·m$^{-3}$. Figure 3 shows that in July 2014, phytoplankton biomass seems to be more important than in September 2015. The NOW is the most productive zone of the studied area [53,54,69]. Following a significant phytoplankton bloom that grows during the months of May and June, the phytoplankton biomass starts to decrease in July and August, then fades slowly from September [51].

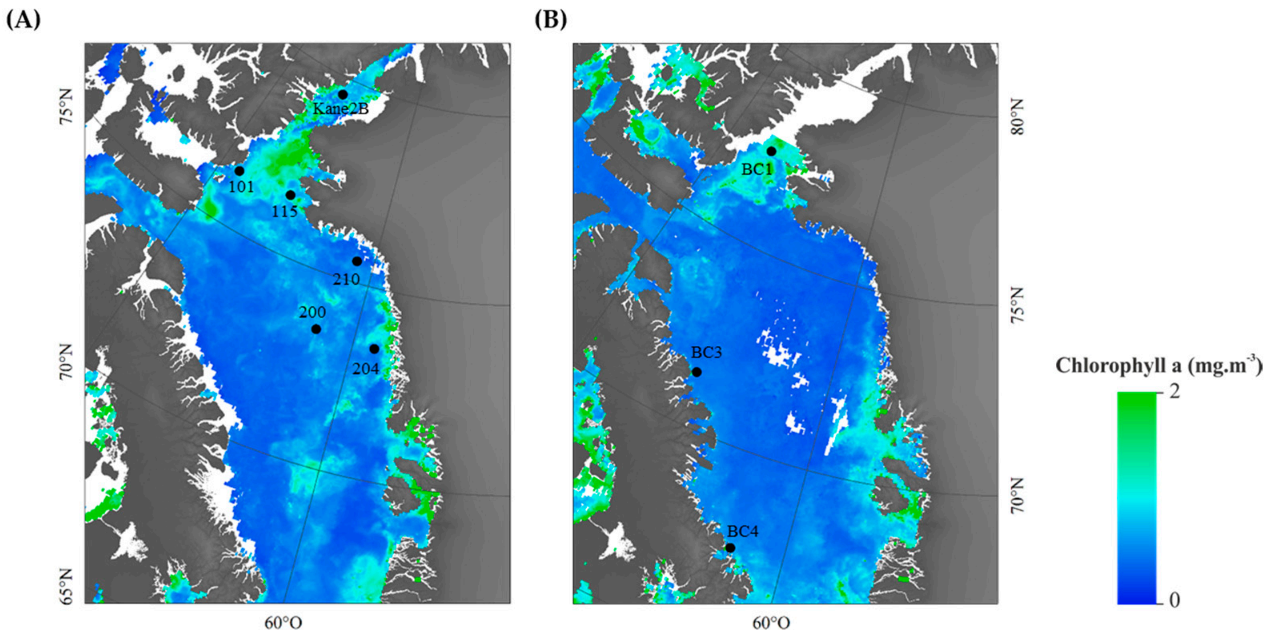


**Figure 3.** Chl. a (mg·m$^{-3}$) monthly concentrations in (**A**) July 2014 and (**B**) September 2015.

Sedimentological and geochemical settings of the sediment measured for this study are shown in Figure 4. Grain-size spectra show all unimodal distribution. In addition, the grain size distribution is consistent for each level of each core. Therefore, we consider the median diameter of the particle size distribution D50 as a reliable measurement of the mean grain size in the sediment cores investigated in the present study. The sediment is mainly muddy–silty. The >125 µm size fraction used for benthic foraminiferal analyses is largely composed of lithic sand, expressing the importance of the ice-rafted transport process in the study area. Only stations 101 and BC1 located in the NOW contain many frustules of diatoms reflecting high primary productivity at the surface.

The NOW area stands out from the rest of the study area with higher TOC and TN contents in the surface sediment. In the Baffin Bay and Nares Strait, the TOC values vary around 1 wt.% and the TN values range from 0.10 to 0.20 wt.% (Figure 4). In the NOW, the TOC contents are >2 wt.% and the TN contents are >0.20 wt.%, reaching 0.33 wt.% at station 101. These values are in line with those measured during the summers of 1998 and 1999 in the same zone by Hamel et al. [70] so we consider them to be representative of average values in this region. Moreover, this study indicates that TOC contents in the surface sediment of the NOW area are significantly higher than those measured in other Arctic or subarctic environments. Our results show that the C/N ratio is equal to eight and nine for all stations except Kane2B where values reaching twelve were measured (Figure 4). Organic matter in surface sediments of the Baffin Bay and Nares Strait mainly originates from primary productivity but includes a little part of terrigenous supply as suggested by the values of the C/N ratio, which are slightly higher to those representatives of marine organic matter (five to seven; [71]). This part is more important in Nares Strait where Holocene sediments are rich in carbon particles from Paleogene series present on the coast of Ellesmere Island [72].

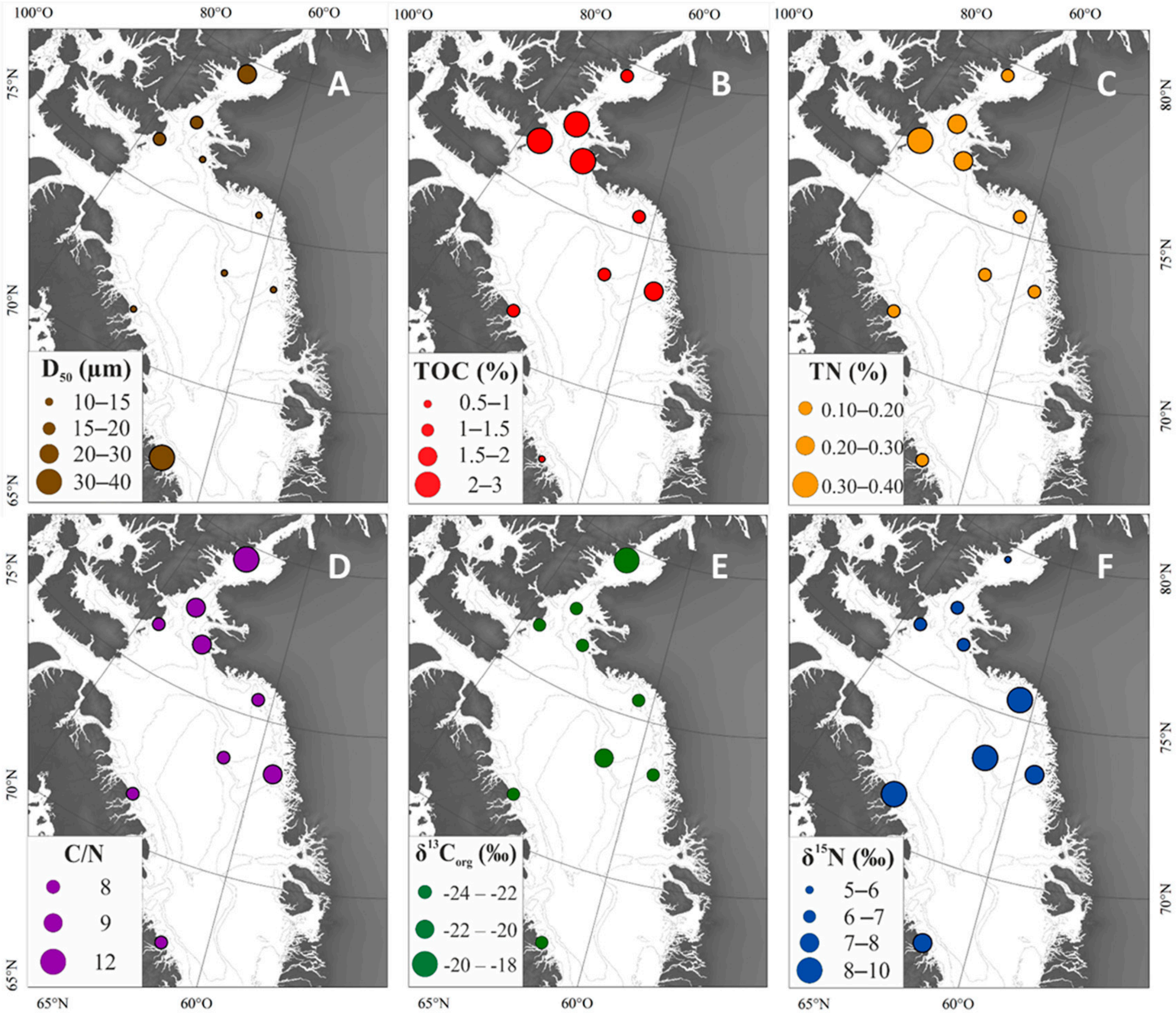


**Figure 4.** Distribution of measured environmental parameters: (**A**) $D_{50}$, (**B**) TOC, (**C**) TN, (**D**) C/N, (**E**) $\delta^{13}C$, and (**F**) $\delta^{15}N$.

$\delta^{13}C_{org}$ is used to indicate the relative importance of marine vs. terrigenous inputs [73] but also changes in $CO_2$ concentration in surface waters [74–76]. In general, marine organic matter is isotopically heavier compared to C3 angiosperm plants (tundra and taiga), which constitute the major part of the Arctic vegetation. The C4 terrestrial plants do not grow in high northern latitudes and so do not contribute to carbon inputs in the Arctic region [77,78]. Our results show that $\delta^{13}C_{org}$ is quite constant in the studied area with values oscillating around −22 and −21‰ (Figure 4). At station Kane2B, $\delta^{13}C_{org}$ is slightly higher, with a value of −19.5‰. Studies by Naidu et al. [79] on carbon stable isotopes in sediments of the Amerasian continental shelf (Bering, Chukchi, Siberian, and Beaufort Seas), allowed us to determine values of terrigenous $\delta^{13}C_{org}$ around −27‰, and −24 to −21‰ for marine $\delta^{13}C_{org}$. According to Pomerleau et al. [80], marine $\delta^{13}C_{org}$ is estimated to be −21‰ in the Baffin Bay region. This value is deduced from the average of $\delta^{13}C_{org}$ of dominant zooplankton species, primary consumers, in the Baffin Bay. According to our results,

$\delta^{13}C_{org}$ values measured in the sediments of the Baffin Bay and NOW stations show a marine origin of organic matter with a slightly terrigenous input similar to what was shown by the s C/N data. Station Kane2B is special, with a higher $\delta^{13}C_{org}$ value (−19.5‰; Figure 4). In the Arctic, algae proliferating under sea ice is a specific element, which can take part in the $\delta^{13}C_{org}$ of the sediment. Indeed, the weak $CO_2$ concentration dissolved in water covered by sea ice leads to an increase in $\delta^{13}C_{org}$ of ice algae. $\delta^{13}C_{org}$ derived from sea ice algae fluctuate around −18‰ [81,82]. The $\delta^{13}C_{org}$ value measured at station Kane2B strongly suggests the presence of sea ice for most of the year in the Nares Strait.

$\delta^{15}N$ measured in sediments is used to trace the relative use of nitrogen ($NO_3^-$) in surface waters, an essential nutrient for primary production [83–85]. It depends on nitrogen isotopic composition in the surface water mass and isotope fractionation from phytoplankton assimilation of nitrogen nutrients. In the photic zone, phytoplankton uses preferentially isotopically weak nitrogen ($^{14}NO_3^-$). In addition, Fox and Walker [86] indicate that sinking particulate organic matter reaches the deep ocean within a few days in the Baffin Bay. We can consider that N is well preserved in surface sediments and that $\delta^{15}N$ provides direct information on primary productivity and nutrient availability in the surface ocean. Our results indicate that $\delta^{15}N$ is slightly different between the Baffin Bay, with values of 7 to 9‰, and the NOW and Nares Strait areas, with weaker values of 5 to 6‰ (Figure 4). Despite it being an intense biological activity in the polynya, nutrient-rich Pacific water from the Arctic Ocean allows the maintenance of relatively weak $\delta^{15}N$ values. On the other hand, $\delta^{15}N$ values measured in sediments of the Baffin Bay are higher, suggesting a lower availability in nutrients in surface waters from the North Atlantic.

### 4.2. Distribution of Living Benthic Foraminifera

The Arctic, particularly in the Baffin Bay, is known to contain numerous species of agglutinated benthic foraminifera [15,17,18,87]. Results of this study are no exception to this rule. Indeed, all studied stations present at least 50% of agglutinated individuals except station BC1 with only 26% (Figure 5A). Stations BC3, 200, 210, 115, and 101 contain the most agglutinated individuals in their respective assemblages (>75%, Supplementary Materials). Station 210 is entirely composed of agglutinated benthic foraminifera.

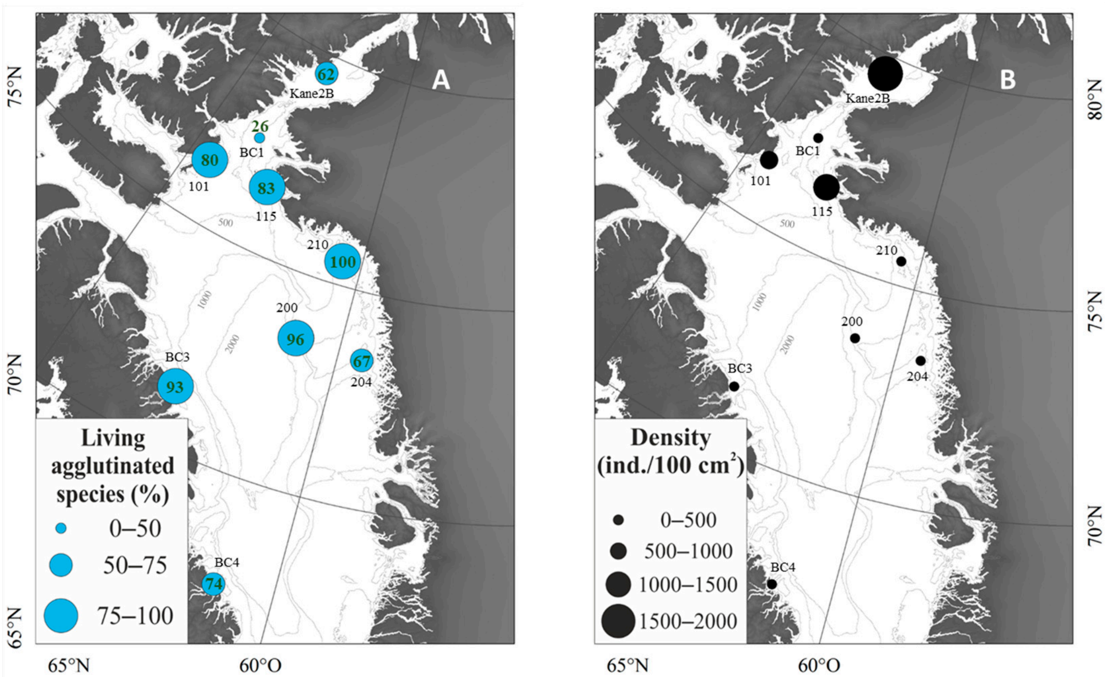


**Figure 5.** (**A**) Proportion of living agglutinated species and (**B**) density of living benthic foraminifera per 100 cm$^2$ for each studied station.

Densities of living fauna for each core expressed in number of individuals per 100 cm$^2$ are shown in Figure 5B and in the middle of the pie charts in Figure 6A. The weakest densities are noticed in the Baffin Bay (150 to 324 ind./100 cm$^2$) and at station BC1 (260 ind./100 cm$^2$). Densities are higher in NOW, with a density higher than 1000 ind./100 cm$^2$ at station 115. The highest density is noticed at station Kane2B with 1754 ind./100 cm$^2$.

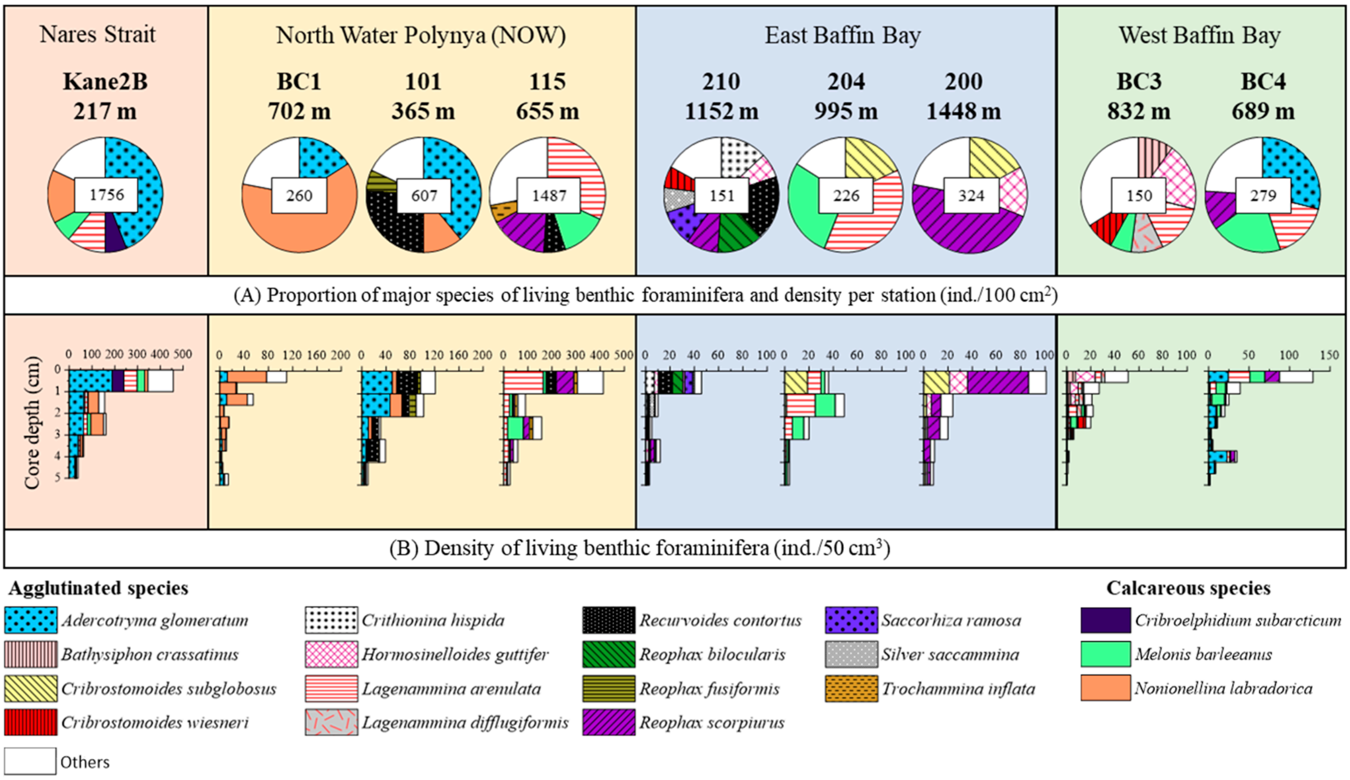


**Figure 6.** (**A**) Proportions of major species of living benthic foraminifera in the first 5 cm of sediment of the cores. Total densities expressed in number of living individuals per 100 cm$^2$ at each station are indicated in the centre of pie charts. (**B**) Vertical distribution in the upper 5 cm of the sediment of major species (>5%) of living benthic foraminifera for the fraction > 125 µm.

For all stations, the relative abundance of major species is illustrated in Figure 6A. Station Kane2B, located in Nares Strait, is dominated by an agglutinated species, *Adercotryma glomeratum* (44%, Figure A1). Another agglutinated species, *Lagenammina arenulata*, is present with a relative abundance of 11%. Calcareous species also compose the assemblage of station Kane2B, such as *Nonionellina labradorica* (15%) and to a lesser extent, *Cribroelphidium subarcticum* and *Melonis barleeanus* (6% each). Species *A. glomeratum* and *N. labradorica* represent a high proportion in the NOW, in cores BC1 (16% and 62%, respectively) and 101 (26% and 11%, respectively). *Recurvoides contortus* (26%) and *Reophax fusiformis* (6%) are associated to these two species in the core 101. The assemblage of station 115 located in the NOW is different from those of the two close stations, 101 and BC1. Major species are similar to those observed in the cores of the Baffin Bay. *Lagenammina arenulata* (32%) is the dominant species at this station. Three other agglutinated species *Reophax scorpiurus* (16%), *R. contortus* (6%), and *Trochammina inflata* (5%), as well as one calcareous species, *M. barleeanus* (13%), complete the assemblage of station 115. In the Baffin Bay, observed species of living benthic foraminifera are largely agglutinated. Therefore, the assemblages are composed of a mix of agglutinated species without any particular trend between the stations. Among others, *Lagenammina arenulata*, *R. scorpiurus*, and *Hormosinelloides guttifer* are found in several cores. *Melonis barleeanus* is the only calcareous species being part of a major species of the Baffin Bay. Species *A. glomeratum* present at stations Kane2B, BC1, and 101 is also found at station BC4, representing 29% of the assemblage.

The vertical distribution of living benthic foraminifera at each station is presented in Figure 6B. The density and the richness are always more important in the first 2 cm of the sediment. The station Kane2B presents the highest surface density with 457 ind./50 $cm^3$. *Adercotryma glomeratum* is found at 5 cm, whereas *N. labradorica* dominates between 1 and 3 cm sediment depth. At station BC1, *N. labradorica* is abundant at the surface then its density decreases to 3 cm. *Adercotryma glomeratum* and *R. contortus* are the most abundant species at station 101. Their densities decrease with depth. The density of *N. labradorica* is more important between 1 and 2 cm. At station 115, *L. arenulata* is the dominant species observed at 5 cm sediment depth. *Melonis barleeanus* is mainly abundant between 2 and 3 cm sediment depth, producing an increase in the density in this sample. Station 210 shows the lowest density together with station BC3. The surface density only reaches 46 ind./50 $cm^3$. The majority of taxa are contained in the first centimeter of the sediment. At station 204, the layer with higher density is found within the 1–2 cm interval contrary to other stations. This observation is due to the presence of *M. barleeanus*, abundant from 1 to 3 cm sediment depth. The three major species of station 200 are grouped together in the topmost layer and the density is raised to 101 ind./50 $cm^3$. *Reophax scorpiurus* is found down to 5 cm. Station BC3 shows a low surface density with 51 ind./50 $cm^3$. Living benthic foraminifera are very rare under 3 cm sediment depth. Station BC4 contains the most important surface density of the Baffin Bay stations with 129 ind./50 $cm^3$. *Melonis barleeanus* is present from the surface to 2 cm sediment depth. A slight increase is visible between 3.5 and 4.5 cm due to the presence of the species *A. glomeratum*.

## 5. Discussion

This study covers a large geographical area, extending from the relatively deep environments of the lower slope in the western and eastern areas of the Baffin Bay to the shallower Kane Basin in Nares Strait, and the unique environment of the NOW connecting those two environments. Environmental settings of the Baffin Bay and Nares Strait appear to be contrasted in term of water masses, phytoplankton productivity, and organic matter fluxes [88] (and references therein). Some authors have already demonstrated the importance of these parameters on the distribution of benthic foraminifera in the Baffin Bay and Canadian Arctic [10–17]. The different water masses and the quantity of organic matter measured in the study area constitute some important features, in addition to some specific features as well as $CO_2$ concentrations in the pore water of the sediment and in the water column, in relation to the export and the degradation of the produced organic matter. This specific environmental context allows an explanation of the repartition of living benthic foraminifera in the region in terms of both richness and density or the assemblage's composition.

### *5.1. Influence of Carbonate Dissolution Process on Assemblages of Benthic Foraminifera*

Agglutinated benthic foraminifera are widely present on the shelves of the Arctic Seas and in the Baffin Bay [18,87]. Several studies reported the dominance of these species in the Canadian Arctic [10–17]. According to these different studies, sea ice cover and properties of water masses would be responsible for the particular distribution of agglutinated benthic foraminifera, establishing a hostile environment for the development of calcareous species as a result of carbonate dissolution in corrosive bottom waters. The shallow CCD in the study area induces carbonate dissolution in the Baffin Bay from 300 m water depth [26]. The sea ice seasonal dynamic favors the absorption of atmospheric $CO_2$ in cold surface waters but also primary productivity therefore increasing the flux of organic matter reaching the ocean floor. Dense and well-oxygenated cold high-latitude waters flowing in the deep ocean oxidize this organic matter leading to a rise of the partial pressure of $CO_2$ in sediment pore waters. High $CO_2$ content at the water–sediment interface causes carbonate dissolution [25,89]. However, in the core BC1 located in the NOW, at approximately 700 m water depth, agglutinated benthic foraminifera only represent 26% of the total of observed living individuals. One calcareous species is largely dominant, *N. labradorica* (62%). This opportunistic species, typical of North Atlantic waters, is a good indicator of high surface productivity which constitute animportant source of organic matter for the benthic community [90–92]. Despite corrosive waters, a number of calcareous individuals (*N. labradorica* and *M. barleeanus* notably) was observed in the cores of the NOW and Kane Basin (200–700 m water depth) but also in the deep environments of the Baffin Bay (to 1000 m water depth). The presence of calcareous species under the CCD could be explained by a seasonal variation of the CCD. At station 204, east of the Baffin Bay, tests of *M. barleeanus* present important marks relating to dissolution (Figure 7). Despite an intense Rose Bengal staining, it could be possible that these individuals have calcified during a period where waters were less corrosive and were later partly dissolved. Considering the depth of station 204 (995 m), the CCD position in the region and the absence of other calcareous species in the core, it would seem that calcification occurs in corrosive conditions. A recent study shows that this species could integrate sedimentary particles during the formation of the calcareous test to strengthen it and to reduce carbonate dissolution [93]. Despite a priori negative conditions, some calcareous species, typically infauna living between 1 and 3 cm sediment depth, can survive and represent an important part of the assemblage of benthic foraminifera in the considered sample (Figure 6).

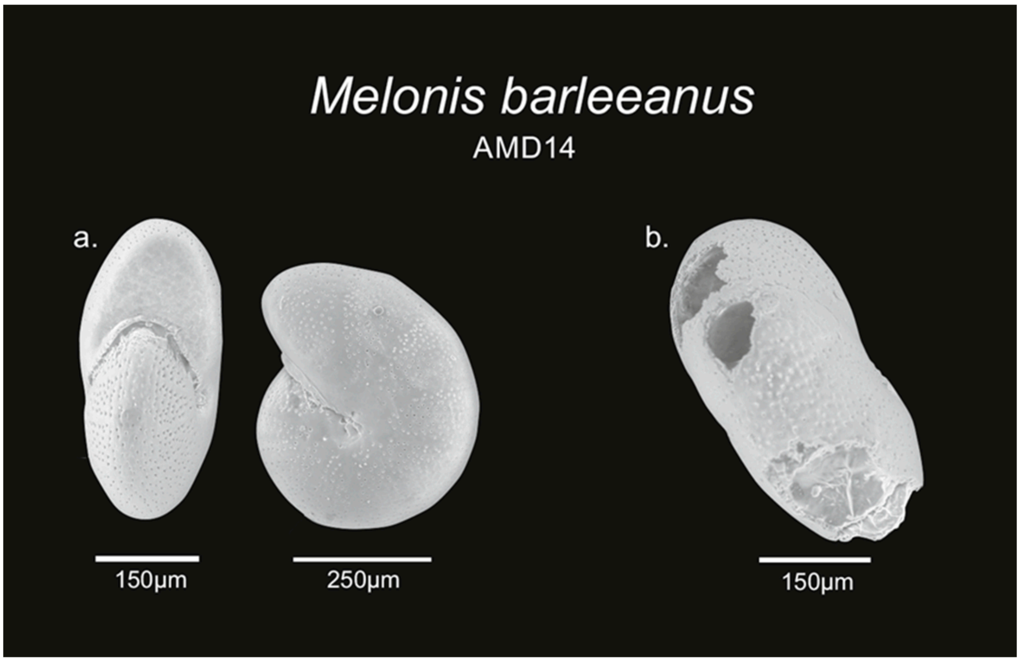


**Figure 7.** Tests of *M. barleeanus* observed in sample of the core Kane2B (**a**) and 204 (**b**) illustrating the difference in the tests' preservation.

The Baffin Bay and Nares Strait present a high diversity of agglutinated species also classically found in the studies about benthic foraminifera in this region of the Canadian Arctic. In this study, species such as *R. scorpiurus*, *L. arenulata*, or *H. guttifer* are largely present in the Baffin Bay, from north to south and from east to west. However, two species appear to have a particular spatial distribution. *Recurvoides contortus* is present in the north of the Baffin Bay, at stations 210, 115, and 101. In some previous studies, this species was observed in the Baffin Bay and Canadian Arctic Archipelago. According to Schröder-Adams and Van Rooyen [16], *R. contortus* would be typical of Atlantic waters of the Baffin Bay. In our study, this species seems to be compatible with particularly cold Atlantic waters north of the Baffin Bay. *Adercotryma glomeratum* is a recurrent species in Nares Strait at stations Kane2B, 101, and BC1 as well as west of the Baffin Bay at station BC4. Schröder-Adams and Van Rooyen [16] observed this species in deep environments of the Baffin Bay particularly (>2000 m water depth) where waters were the coldest. *Adercotryma glomeratum* is a common species, in the high latitudes and in cold waters of the North Atlantic and Arctic Oceans [14–16,94]. In our study, this species is primarily present in Nares Strait and the western part of the Baffin Bay, as a consequence of the inflow of cold waters from the Arctic Ocean.

In good agreement with previous observations, a large part of living benthic foraminifera observed in this study are agglutinated. The association of different parameters such as seasonal sea ice cover as well as the flux of organic matter and cold temperatures lead to the corrosive nature of water masses in the region. Carbonate dissolution appears to be an important controlling factor on benthic fauna but cannot totally explain the distribution of living benthic foraminifera in the study area.

### 5.2. Relation between Primary Productivity and Distribution of Benthic Foraminifera

The distribution of living benthic foraminifera is influenced by various biotic and abiotic parameters among which the oxygenation of deep waters and the supply of organic matter exert important control on fauna [95–98]. In Arctic environments, in areas of dense water formation, the oxygenation of deep waters is rarely a restricting factor. Therefore, the flux and the quality of organic matter are dominant factors controlling the distribution of benthic foraminifera.

The highest densities of living benthic foraminifera in this study were observed in the Kane Basin with 1456 ind./100 $cm^2$ and in the NOW (1487 ind./100 $cm^2$). The highest densities in the NOW are consistent with observations of high productivity in this area [52,53,99] related to a combination of physical factors such as light availability, water masses stratification, and vertical mixing, and nutrient advection in the photic layer. However, it is worth noting that a certain disparity between the densities of living fauna was observed at the three stations of the NOW. On the one hand, there is a clear difference in faunal density between station 115 on the east (1487 ind./100 $cm^2$) and station 101 on the west( 607 ind./100 $cm^2$) of the polynya, although they were bothsampled in July 2014. This observation confirms the disparity of primary productivity, being earlier and more active to the east [57,100] due to particular physical conditions (e.g., SST, sea ice, and stratification). Burger et al. [100], presenting the results of chlorophyll a measurements collected during the same scientific cruise in July 2014, explains the observed summer phytoplankton bloom by deep-water upwelling phenomena providing nutrients to fuel the bloom. On the other hand, station BC1, in the central part of the polynya, presents the lowest density observed in the NOW area (260 ind./100 $cm^2$). This is probably related to the sampling period. Indeed, sediments of the station BC1 were collected early in the fall when the polynya, largely open on the Baffin Bay, is no longer really a strict polynya [53]. In fall, primary productivity is lower than in summer due to water masses stratification and a drop in solar irradiance at the surface of the water, significantly restricting the export of food to the bottom. Regarding station Kane2B, environmental conditions are different as the Kane Basin is located beyond the ice bridge marking the northern limit of the NOW. Nevertheless, a maximum density of living benthic foraminifera in this study can be observed here. While the TOC content remains rather low at this station, the C/N ratio reveals labile properties. Nutrient availability brought by cold Artic water leads to relatively important productivity in this region. Moreover, $\delta^{13}C_{org}$ measured in the surface sediment of this core indicates an export of sea ice algae feeding the benthic food chain in the Kane Basin. MODIS Terra satellite images (Figure 8) show that the situation in the Kane Basin in July 2014 is quite atypical compared to the same period in 2013 and 2015. Indeed, sea ice broke up earlier during the summer of 2014, resembling conditions of polynya type. Burgers et al. [100] also observed a sub-surface phytoplankton bloom in the Kane Basin during summer of 2014 above a topographic feature causing the formation of a localized upwelling and a supply of nutrients that fed the bloom. In the Baffin Bay, observed densities of living benthic foraminifera in surface sediments do not present notable variations between the east and west despite contrasting environmental features in terms of water masses, sea ice cover, or phytoplankton biomass. However, densities of living benthic foraminifera are significantly lower than in Nares Strait. $\delta^{15}N$ measurements in the sediment indicate lower nutrient availability in North Atlantic waters flowing in the Baffin Bay. Primary productivity is less intense than in the NOW and this is reflected in recorded densities in this study.

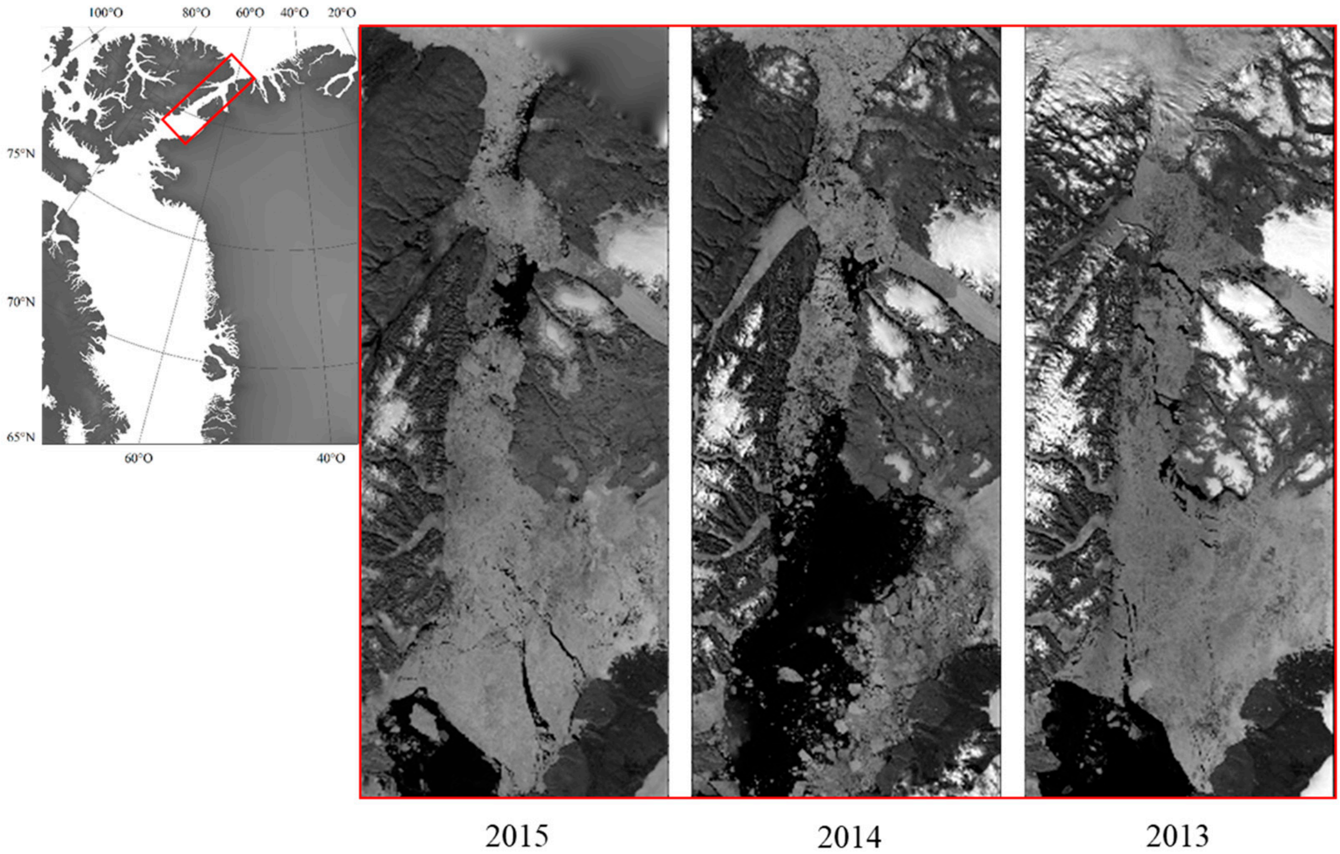


**Figure 8.** Sea ice cover in Nares Strait in July 2015 (**left**), 2014 (**middle**), and 2013 (**right**) from satellite images MODIS Terra. Note the unusual situation during the summer of 2014 with the Kane Basin being relatively free of ice.

Observed densities of living benthic foraminifera in the study area seem to be in line with locally measured Chl. a concentrations in July 2014 and September 2015 at the sampling stations. The flux of organic matter would be a key parameter for the proliferation of species of benthic foraminifera in the Baffin Bay and Nares Strait regions.

As well as faunal densities, assemblages of benthic foraminifera show some large geographical disparities. Two main assemblages characterize the populations of benthic foraminifera in this study. The first assemblage is dominated by the species *N. labradorica* and *A. glomeratum*. The second assemblage is essentially composed of an assortment of agglutinated species sometimes associated with the calcareous species *M. barleeanus*. In the Kane Basin, the major species, *A. glomeratum*, indicates the presence of cold Arctic waters, while the species *N. labradorica* and *M. barleeanus* highlight the export and the availability of organic matter in the benthic environment [97,98,101,102]. Observed species of living benthic foraminifera in the cores of the NOW distinguish themselves by two different assemblages between the east and west of the polynya, at the mouth of Nares Strait. Indeed, stations BC1 and 101, to the east, are characterized by the abundance of species *A. glomeratum* and *N. labradorica*, while station 115, to the west, shows a more important number of species but that are mostly agglutinated. *Adercotryma glomeratum* highlights cold waters flowing down to the south along Ellesmere Island in Nares Strait. The NOW is considered to be the most productive region of the Arctic despite a drastic reduction in productivity and phytoplankton biomass revealed by several recent studies [51,56–58]. The spring bloom starts at the end of April or the beginning of May, and east of the polynya, along the Greenland coast, due to the early sea ice retreat generated by relatively warm Atlantic water moving through the WGC [51]. The living benthic foraminiferal assemblage at station 115 is mostly composed of agglutinated species also found in the cores of the Baffin Bay, highlighting the influence of this corrosive Atlantic water mass. The presence of the intermediate infauna *M. barleeanus*, indicates that the organic matter available in this area and during that period is relatively degraded [91,97,98,101,103]. The phytoplankton bloom occurs later, west of the polynya, at the beginning of June [51]. At stations BC1 and 101 sampled in October and July, respectively, *N. labradorica* is abundant. This species is associated with episodic production of fresh phytodetritus in areas of high seasonal productivity [102,104,105], indicating the existence of a spring phytoplankton bloom then a less intense fall bloom.

The distinctive characteristic of the benthic assemblages of the Baffin Bay, south of the NOW, is the dominance of agglutinated species. The only living observed calcareous species in the cores of this region is *M. barleeanus*, an indicator species of relatively degraded organic matter in the sediment of the Baffin Bay. Between the east and the west of the Baffin Bay, faunas do not show any clear differences in terms of species or abundance. This is attributable to the fact that at the sampling depth of the cores in the Baffin Bay (from 689 m depth to 1448 m depth), the Atlantic water mass is dominant. However, the presence of the cold-water indicator species, *A. glomeratum*, at station BC4 would indicate the influence of Arctic waters carried by the BC. Environmental conditions in the Baffin Bay are relatively stable in summer and fall. A sampling earlier in the season might have allowed us to highlight changes in the composition of benthic foraminiferal assemblages, following sea ice retreat initiated from the east and later to the west of the Baffin Bay.

Living benthic foraminiferal assemblages in general appear to be closely linked to the different dominant water masses in the Baffin Bay and Nares Strait. Faunal density and diversity, as well as assemblages, reflect the relation between pelagic and benthic environments in this high-latitude environment, despite the presence of sea ice for most of the year. Particularly, high densities in Nares Strait (NOW and Kane Basin) highlight the connection between primary productivity, the flux of organic matter, and the quality of the available organic matter and the benthic life in such extreme environments. Some benthic foraminifera taxa clearly respond better to food supply in those environments.

## 6. Conclusions

This study provides some important information about the ecology of benthic foraminifera in the Baffin Bay and Nares Strait. Assemblages of living benthic foraminifera are associated with specific environments of the studied area. Features of water masses and especially their corrosive nature, as well as primary productivity and the associated flux of organic matter, are essential parameters influencing the distribution of benthic foraminifera. Carbonate dissolution is also a major influencing factor on faunas of benthic foraminifera in the Baffin Bay and explain the dominance of agglutinated taxa over calcareous taxa in the area. Living faunal density is closely linked with the flux of organic matter produced in surface water. This phenomenon is clearly illustrated with regard to the important differences between the lowest density measured in the Baffin Bay and those observed in the NOW. Moreover, particular species are sensitive to the quantity and quality of available organic matter in benthic environments. In particular, species *N. labradorica* responds quickly and massively to episodic food supply, while *M. barleeanus* tolerates environments where organic matter is more degraded.

More knowledge on the ecology of benthic foraminifera living in complex environments subject to seasonal sea ice cover is essential for optimal use of these fauna as a paleoenvironmental proxy in Arctic regions.

**Supplementary Materials:** The following supporting information can be downloaded at: https://www.mdpi.com/article/10.3390/jmse11112049/s1. Raw counting data for benthic foraminifera (>125 μm) in all stations.

**Author Contributions:** Conceptualization, J.B. and C.R.; methodology, J.B., C.R. and P.-A.D.; validation, J.B., C.R., J.G. and P.-A.D.; formal analysis, C.R. and P.-A.D.; investigation, J.B., C.R. and J.G.; resources, J.B. and C.R.; data curation, J.B., C.R. and P.-A.D.; writing—original draft preparation, J.B., C.R., J.G. and P.-A.D.; writing—review and editing, C.R. and J.B.; visualization, C.R.; supervision, J.B. and J.G.; project administration, J.B.; funding acquisition, J.B. All authors have read and agreed to the published version of the manuscript.

**Funding:** The cores and material used in this study were collected during the AMD14 and AMD15 oceanographic campaigns on board the NGGC Amundsen as part of the GreenEdge project funded by ANR and the Total Foundation. Expedition time was funded by the ERC-STGICEPROXY project. The research presented in this manuscript is part of the ICCAR project funded by the French INSU-CYBER Program.

**Institutional Review Board Statement:** Not applicable.

**Informed Consent Statement:** Not applicable.

**Data Availability Statement:** All relevant data are shown in the Supplementary Materials.

**Acknowledgments:** We thank the captain, officers and crew of the NGCC *Amundsen* for their support during the 2014 and 2015 ArcticNet cruises.

**Conflicts of Interest:** The authors declare no conflict of interest. The funders had no role in the design of the study; in the collection, analyses, or interpretation of data; in the writing of the manuscript; or in the decision to publish the results.

## Appendix A

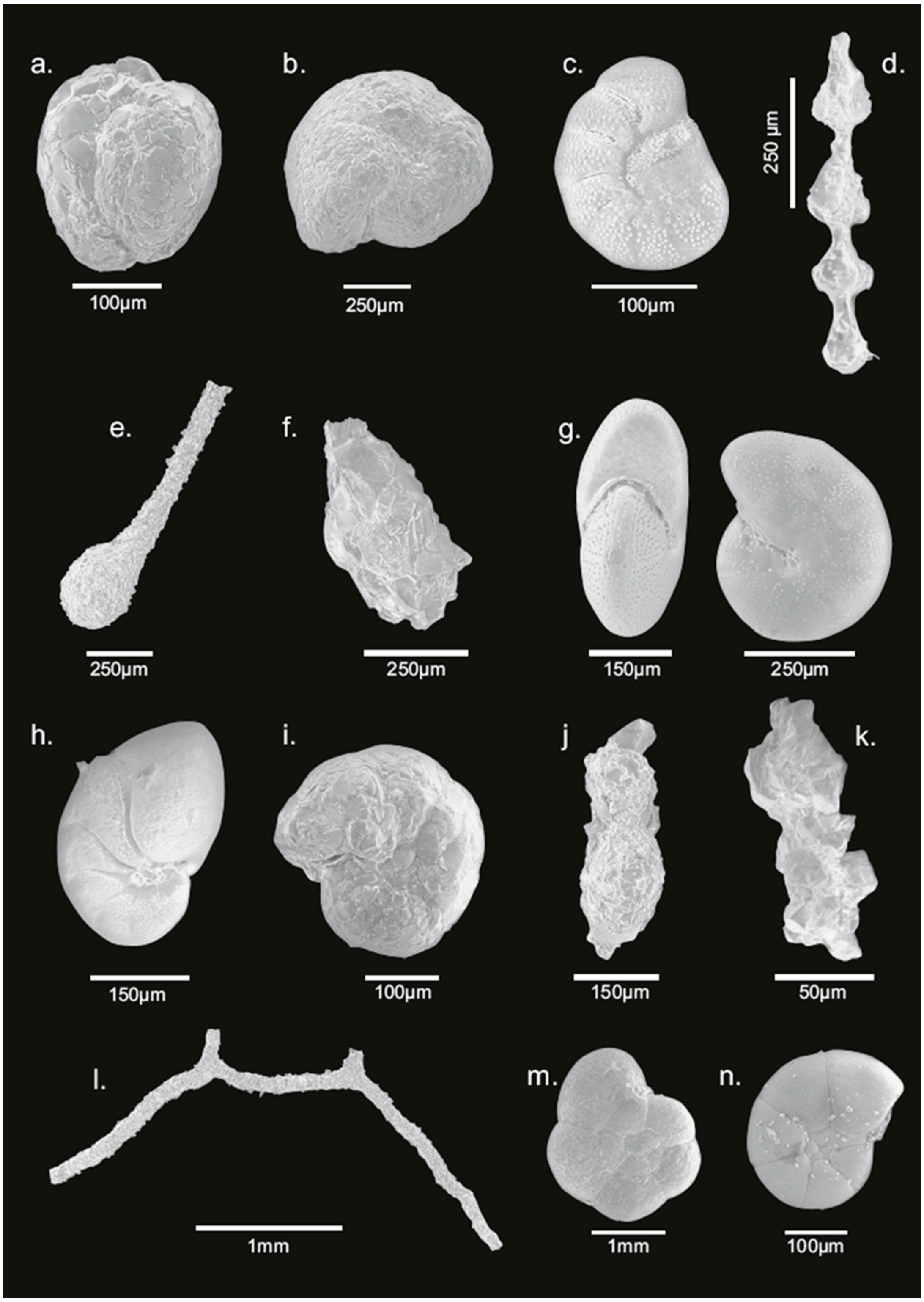


**Figure A1.** Plate of SEM photographs of the major species. (**a**): *Adercotryma glomeratum*; (**b**): *Cribrostomoides subglobosus*; (**c**): *Cribroelphidium subarcticum*; (**d**): *Hormosinelloides guttifer*; (**e**,**l**): *Saccorhiza ramosa*; (**f**): *Lagenammina arenulata*; (**g**): *Melonis barleeanus*; (**h**): *Nonionellina labradorica*; (**i**): *Recurvoides contortus*; (**j**): *Reophax bilocularis*; (**k**): *Reophax scorpiurus*; (**m**): *Trochammina inflata*; and (**n**): *Cribrostomoides weisneri*.

## Appendix B. Taxonomic References List

*Adercotryma glomeratum* (Brady, 1878)
*Allogromiida* sp. (Loeblich and Tappan, 1961)
*Ammoglobigerina globigeriniformis* (Parker and Jones, 1865)
*Ammotium cassis* (Parker, 1870)
*Arenoturrispirillina catinus* (Höglund, 1947)
*Astrononion stellatum* (Terquem, 1882)
*Bathysiphon crassatinus* (Brady, 1881)
*Bolivina* sp. (d'Orbigny, 1839)
*Buccella frigida* (Cushman, 1922)
*Cassidulina reniforme* (Nørvang, 1945)
*Cassidulina teretis* (Tappan, 1951)
*Cornuspira involvens* (Reuss, 1850)
*Cribroelphidium subarcticum* (Cushman, 1944)
*Cribrostomoides subglobosus* (Cushman, 1910)
*Cribrostomoides wiesneri* (Parr, 1950)
*Crithionina hispida* (Flint, 1899)
*Eggerelloides advena* (Cushman, 1922)
*Elphidium excavatum* (Terquem, 1875)
*Glandulina ovula* (d'Orbigny, 1846)
*Globobulimina pyrula* (d'Orbigny, 1846)
*Hormosinelloides guttifer* (Brady, 1881)
*Hyalinonetrion gracillimum* (Seguenza, 1862)
*Hyperammina elongata* (Brady, 1878)
*Islandiella helenae* (Feyling-Hanssen and Buzas, 1976)
*Islandiella norcrossi* (Cushman, 1933)
*Labrospira crassimargo* (Norman, 1892)
*Laevidentalina haueri* (Neugeboren, 1856)
*Lagenammina arenulata* (Skinner, 1961)
*Lagenammina difflugiformis* (Brady, 1879)
*Lagenammina tubulata* (Rhumbler, 1931)
*Lagenammina* spp. (Rhumbler, 1911)
*Lenticulina* sp. (Lamarck, 1804)
*Lobatula lobatula* (Walker and Jacob, 1798)
*Melonis barleeanus* (Williamson, 1858) = *Melonis affinis* (Reuss, 1851)
*Miliammina fusca* (Brady, 1870)
*Nonionella stella* (Cushman and Moyer, 1930)
*Nonionellina labradorica* (Dawson, 1860)
*Nonionoides turgidus* (Williamson, 1858)
*Portatrochammina karica* (Shchedrina, 1946)
*Pseudonodosinella nodulosa* (Brady, 1879)
*Pullenia bulloides* (d'Orbigny, 1846)
*Pyrgo williamsoni* (Silvestri, 1923)
*Pyrgo* sp. (Defrance, 1824)
*Quinqueloculina* sp. (d'Orbigny, 1826)
*Recurvoides contortus* (Earland, 1934)
*Recurvoides turbinatus* (Brady, 1881)
*Reophax bilocularis* (Flint, 1899)
*Reophax fusiformis* (Williamson, 1858)
*Reophax scorpiurus* (Montfort, 1808)
*Reussoolina laevis* (Montagu, 1803)
*Rhizammina algaeformis* (Brady, 1879)
*Robertinoides charlottensis* (Cushman, 1925)
*Saccammina* sp. Sars in Carpenter, 1869
*Saccorhiza ramosa* (Brady, 1879)
Silver saccamminid (Gooday et al., 2005)
*Spiroplectammina biformis* (Parker and Jones, 1865)

*Stainforthia concava* (Höglund, 1947)
*Thurammina* sp. (Brady, 1879)
*Triloculina oblonga* (Montagu, 1803)
*Triloculina trihedra* (Loeblich and Tappan, 1953)
*Trochammina inflata* (Montagu, 1808)
*Trochammina nana* (Brady, 1881)
*Uvigerina* sp. (d'Orbigny, 1826)
*Verneuilinulla affixa* (Cushman, 1911)

## References


1. Johannessen, O.M.; Bengtsson, L.; Miles, M.W.; Kuzmina, S.I.; Semenov, V.A.; Alekseev, G.V.; Nagurnyi, A.P.; Zakharov, V.F.; Bobylev, L.P.; Pettersson, L.H.; et al. Arctic climate change: Observed and modelled temperature and sea-ice variability. *Tellus Dyn. Meteorol. Oceanogr.* **2004**, *56*, 328–341. [CrossRef]
2. Box, J.E.; Colgan, W.T.; Christensen, T.R.; Schmidt, N.M.; Lund, M.; Parmentier, F.-J.W.; Brown, R.; Bhatt, U.S.; Euskirchen, E.S.; Romanovsky, V.E.; et al. Key indicators of Arctic climate change: 1971–2017. *Environ. Res. Lett.* **2019**, *14*, 045010. [CrossRef]
3. Overland, J.; Dunlea, E.; Box, J.E.; Corell, R.; Forsius, M.; Kattsov, V.; Olsen, M.S.; Pawlak, J.; Reiersen, L.-O.; Wang, M. The urgency of Arctic change. *Polar Sci.* **2019**, *21*, 6–13. [CrossRef]
4. AR6 Synthesis Report: Climate Change 2023—IPCC. Available online: https://www.ipcc.ch/report/sixth-assessment-report-cycle/ (accessed on 18 September 2023).
5. Arctic Monitoring and Assessment Programme (AMAP). *AMAP Assessment 2018: Arctic Ocean Acidification*; Report; Arctic Monitoring and Assessment Programme (AMAP): Tromso, Norway, 2018. [CrossRef]
6. Brown, T.A.; Galicia, M.P.; Thiemann, G.W.; Belt, S.T.; Yurkowski, D.J.; Dyck, M.G. High contributions of sea ice derived carbon in polar bear (Ursus maritimus) tissue. *PLoS ONE* **2018**, *13*, e0191631. [CrossRef]
7. Kushner, P.J.; Mudryk, L.R.; Merryfield, W.; Ambadan, J.T.; Berg, A.; Bichet, A.; Brown, R.; Derksen, C.; Déry, S.J.; Dirkson, A.; et al. Canadian snow and sea ice: Assessment of snow, sea ice, and related climate processes in Canada's Earth system model and climate-prediction system. *Cryosphere* **2018**, *12*, 1137–1156. [CrossRef]
8. Jahn, A.; Holland, M.M. Implications of Arctic sea ice changes for North Atlantic deep convection and the meridional overturning circulation in CCSM4-CMIP5 simulations. *Geophys. Res. Lett.* **2013**, *40*, 1206–1211. [CrossRef]
9. Loder, J.W.; van der Baaren, A.; Yashayaev, I. Climate Comparisons and Change Projections for the Northwest Atlantic from Six CMIP5 Models. *Atmosphere-Ocean* **2015**, *53*, 529–555. [CrossRef]
10. Phleger, F.B. *Foraminifera Distribution in Some Sediment Samples from the Canadian and Greenland Arctic Cushman Foundation Foraminifer Research Contribution*; Scripps Institution of Oceanography, University of California: San Diego, CA, USA, 1952; Volume 3.
11. Marlowe, J.I.; Vilks, G. *Marine Geology, Eastern Part of Prince Gustaf Adolf Sea, District of Franklin: Polar Continental Shelf Project*; Department of Mines and Technical Surveys: Ottawa, ON, Canada, 1963; Volume 63.
12. Vilks, G. *Foraminiferal Study of East Bay, Mackenzie King Island, District of Franklin: Polar Continental Shelf Project*; Department of Mines and Technical Surveys: Ottawa, ON, Canada, 1964; Volume 64.
13. Vilks, G. Recent Foraminifera in the Canadian Arctic. *Micropaleontology* **1969**, *15*, 35–60. [CrossRef]
14. Hunt, A.S.; Corliss, B.H. Distribution and microhabitats of living (stained) benthic foraminifera from the Canadian Arctic Archipelago. *Mar. Micropaleontol.* **1993**, *20*, 321–345. [CrossRef]
15. Lloyd, J.M. Modern distribution of benthic foraminifera from Disko Bugt, West Greenland. *J. Foraminifer. Res.* **2006**, *36*, 315–331. [CrossRef]
16. Schroeder-Adams, C.J.; Van Rooyen, D. Response of Recent Benthic Foraminiferal Assemblages to Contrasting Environments in Baffin Bay and the Northern Labrador Sea, Northwest Atlantic. *Arctic* **2011**, *64*, 317–341. [CrossRef]
17. Schroder-Adams, C.J.; Cole, F.E.; Medioli, F.S.; Mudie, P.J.; Scott, D.B.; Dobbin, L. Recent Arctic shelf foraminifera; seasonally ice covered vs. perennially ice covered areas. *J. Foraminifer. Res.* **1990**, *20*, 8–36. [CrossRef]
18. Wollenburg, J.; Kuhnt, W. The response of benthic foraminifers to carbon flux and primary production in the Arctic Ocean. *Mar. Micropaleontol.* **2000**, *40*, 189–231. [CrossRef]
19. Knudsen, K.L.; Stabell, B.; Seidenkrantz, M.; Eiríksson, J.; Blake, W. Deglacial and Holocene conditions in northernmost Baffin Bay: Sediments, foraminifera, diatoms and stable isotopes. *Boreas* **2008**, *37*, 346–376. [CrossRef]
20. Mudie, P.J.; Rochon, A.; Prins, M.A.; Soenarjo, D.; Troelstra, S.R.; Levac, E.; Scott, D.B.; Roncaglia, L.; Kuijpers, A. Late Pleistocene-Holocene Marine Geology of Nares Strait region: Paleoceanography from foraminifera and dinoflagellate cysts, sedimentology and stable isotopes. *Polarforschung* **2006**, *74*, 169–183.
21. Osterman, L.E.; Nelson, A.R. Latest Quaternary and Holocene paleoceanography of the eastern Baffin Island continental shelf, Canada: Benthic foraminiferal evidence. *Can. J. Earth Sci.* **1989**, *26*, 2236–2248. [CrossRef]
22. Seidenkrantz, M.-S. Benthic foraminifera as palaeo sea-ice indicators in the subarctic realm—Examples from the Labrador Sea–Baffin Bay region. *Quat. Sci. Rev.* **2013**, *79*, 135–144. [CrossRef]

23. Seidenkrantz, M.-S.; Aagaard-Sørensen, S.; Sulsbrück, H.; Kuijpers, A.; Jensen, K.; Kunzendorf, H. Hydrography and climate of the last 4400 years in a SW Greenland fjord: Implications for Labrador Sea palaeoceanography. *Holocene* **2007**, *17*, 387–401. [CrossRef]
24. Aksu, A.E.; Piper, D.J. Baffin Bay in the past 100,000 yr. *Geology* **1979**, *7*, 245–248. [CrossRef]
25. De Vernal, A.; Bilodeau, G.; Hillaire-Marcel, C.; Kassou, N. Quantitative assessment of carbonate dissolution in marine sediments from foraminifer linings vs. shell ratios: Davis Strait, northwest North Atlantic. *Geology* **1992**, *20*, 527–530. [CrossRef]
26. Aksu, A. Holocene and Pleistocene dissolution cycles in deep-sea cores of Baffin Bay and Davis Strait: Palaeoceano-graphic implications. *Mar. Geol.* **1983**, *53*, 331–348. [CrossRef]
27. Cuny, J.; Rhines, P.B.; Kwok, R. Davis Strait volume, freshwater and heat fluxes. *Deep Sea Res. Part Oceanogr. Res. Pap.* **2005**, *52*, 519–542. [CrossRef]
28. Tang, C.C.; Ross, C.K.; Yao, T.; Petrie, B.; DeTracey, B.M.; Dunlap, E. The circulation, water masses and sea-ice of Baffin Bay. *Prog. Oceanogr.* **2004**, *63*, 183–228. [CrossRef]
29. Solignac, S.; Seidenkrantz, M.-S.; Jessen, C.; Kuijpers, A.; Gunvald, A.K.; Olsen, J. Late-Holocene sea-surface conditions offshore Newfoundland based on dinoflagellate cysts. *Holocene* **2011**, *21*, 539–552. [CrossRef]
30. Perrette, M.; Yool, A.; Quartly, G.D.; Popova, E.E. Near-ubiquity of ice-edge blooms in the Arctic. *Biogeosciences* **2011**, *8*, 515–524. [CrossRef]
31. Sakshaug, E. Primary and Secondary Production in the Arctic Seas. In *The Organic Carbon Cycle in the Arctic Ocean*; Stein, R., Macdonald, R.W., Eds.; Springer: Berlin/Heidelberg, Germany, 2004; pp. 57–81.
32. Grebmeier, J.M.; Barry, J.P. The influence of oceanographic processes on pelagic-benthic coupling in polar regions: A benthic perspective. *J. Mar. Syst.* **1991**, *2*, 495–518. [CrossRef]
33. Morata, N.; Renaud, P.; Brugel, S.; Hobson, K.; Johnson, B. Spatial and seasonal variations in the pelagic–benthic coupling of the southeastern Beaufort Sea revealed by sedimentary biomarkers. *Mar. Ecol. Prog. Ser.* **2008**, *371*, 47–63. [CrossRef]
34. Wassmann, P. Sedimentation and benthic mineralization of organic detritus in a Norwegian fjord. *Mar. Biol.* **1984**, *83*, 83–94. [CrossRef]
35. Jensen, H.M.; Pedersen, L.; Burmeister, A.; Hansen, B.W. Pelagic primary production during summer along 65 to 72°N off West Greenland. *Polar Biol.* **1999**, *21*, 269–278. [CrossRef]
36. Platt, T.; Harrison, W.; Irwin, B.; Horne, E.P.; Gallegos, C.L. Photosynthesis and photoadaptation of marine phytoplankton in the arctic. *Deep Sea Res. Part Oceanogr. Res. Pap.* **1982**, *29*, 1159–1170. [CrossRef]
37. Kliem, N.; Greenberg, D.A. Diagnostic simulations of the summer circulation in the Canadian arctic archipelago. *Atmosphere-Ocean* **2003**, *41*, 273–289. [CrossRef]
38. Münchow, A.; Melling, H.; Falkner, K.K. An Observational Estimate of Volume and Freshwater Flux Leaving the Arctic Ocean through Nares Strait. *J. Phys. Oceanogr.* **2006**, *36*, 2025–2041. [CrossRef]
39. Münchow, A.; Falkner, K.K.; Melling, H. Spatial continuity of measured seawater and tracer fluxes through Nares Strait, a dynamically wide channel bordering the Canadian Archipelago. *J. Mar. Res.* **2007**, *65*, 759–788. [CrossRef]
40. Rabe, B.; Johnson, H.L.; Münchow, A.; Melling, H. Geostrophic ocean currents and freshwater fluxes across the Canadian polar shelf via Nares Strait. *J. Mar. Res.* **2012**, *70*, 603–640. [CrossRef]
41. Samelson, R.M.; Barbour, P. *Mesoscale Dynamics and Orographic Channeling of Low-Level Flow through Nares Strait*; Oregon State University: Corvallis, CO, USA, 2006.
42. Jennings, A.; Sheldon, C.; Cronin, T.; Francus, P.; Stoner, J.; Andrews, J. The Holocene History of Nares Strait: Transition from Glacial Bay to Arctic-Atlantic Throughflow. *Oceanography* **2011**, *24*, 26–41. [CrossRef]
43. Bailey, W.B. Oceanographic Features of the Canadian Archipelago. *J. Fish. Board Can.* **1957**, *14*, 731–769. [CrossRef]
44. Melling, H.; Gratton, Y.; Ingram, G. Ocean circulation within the North Water polynya of Baffin Bay. *Atmosphere-Ocean* **2001**, *39*, 301–325. [CrossRef]
45. Barber, D.; Marsden, R.; Minnett, P.; Ingram, G.; Fortier, L. Physical processes within the North Water (NOW) polynya. *Atmosphere-Ocean* **2001**, *39*, 163–166. [CrossRef]
46. Lewis, E.L.; Ponton, D.; Legendre, L.; Leblanc, B. Springtime sensible heat, nutrients and phytoplankton in the Northwater Polynya, Canadian Arctic. *Cont. Shelf Res.* **1996**, *16*, 1775–1792. [CrossRef]
47. Fortier, L.; Fortier, M.; Fukuchi, M.; Barber, D.; Gratton, Y.; Legendre, L.; Odate, T.; Hargrave, B. The International North Water Polynya Study (NOW): A Progress Report (Scientific Note). *Mem. Natl. Inst. Polar Res. Spec. Issue* **2001**, *54*, 343–348.
48. Ingram, R.; Bâcle, J.; Barber, D.G.; Gratton, Y.; Melling, H. An overview of physical processes in the North Water. *Deep Sea Res. Part II Top. Stud. Oceanogr.* **2002**, *49*, 4893–4906. [CrossRef]
49. Tremblay, J.; Hattori, H.; Michel, C.; Ringuette, M.; Mei, Z.-P.; Lovejoy, C.; Fortier, L.; Hobson, K.A.; Amiel, D.; Cochran, K. Trophic structure and pathways of biogenic carbon flow in the eastern North Water Polynya. *Prog. Oceanogr.* **2006**, *71*, 402–425. [CrossRef]
50. Vincent, R.F. A Study of the North Water Polynya Ice Arch using Four Decades of Satellite Data. *Sci. Rep.* **2019**, *9*, 20278. [CrossRef]
51. Marchese, C.; Albouy, C.; Tremblay, J.; Dumont, D.; D'ortenzio, F.; Vissault, S.; Bélanger, S. Changes in phytoplankton bloom phenology over the North Water (NOW) polynya: A response to changing environmental conditions. *Polar Biol.* **2017**, *40*, 1721–1737. [CrossRef]
52. Klein, B.; LeBlanc, B.; Mei, Z.-P.; Beret, R.; Michaud, J.; Mundy, C.-J.; von Quillfeldt, C.H.; Garneau, M.; Roy, S.; Gratton, Y.; et al. Phytoplankton biomass, production and potential export in the North Water. *Deep Sea Res. Part II Top. Stud. Oceanogr.* **2002**, *49*, 4983–5002. [CrossRef]

53. Tremblay, J.; Gratton, Y.; Carmack, E.C.; Payne, C.D.; Price, N.M. Impact of the large-scale Arctic circulation and the North Water Polynya on nutrient inventories in Baffin Bay. *J. Geophys. Res. Ocean.* **2002**, *107*, 26–1–26–14. [CrossRef]
54. Tremblay, J.-E.; Gratton, Y.; Fauchot, J.; Price, N.M. Climatic and oceanic forcing of new, net, and diatom production in the North Water. *Deep Sea Res. Part II Top. Stud. Oceanogr.* **2002**, *49*, 4927–4946. [CrossRef]
55. Kwok, R.; Pedersen, L.T.; Gudmandsen, P.; Pang, S.S. Large sea ice outflow into the Nares Strait in 2007. *Geophys. Res. Lett.* **2010**, *37*, L03502. [CrossRef]
56. Bélanger, S.; Babin, M.; Tremblay, J. Increasing cloudiness in Arctic damps the increase in phytoplankton primary production due to sea ice receding. *Biogeosciences* **2013**, *10*, 4087–4101. [CrossRef]
57. Bergeron, M.; Tremblay, J. Shifts in biological productivity inferred from nutrient drawdown in the southern Beaufort Sea (2003-2011) and northern Baffin Bay (1997–2011), Canadian Arctic. *Geophys. Res. Lett.* **2014**, *41*, 3979–3987. [CrossRef]
58. Blais, M.; Ardyna, M.; Gosselin, M.; Dumont, D.; Bélanger, S.; Tremblay, J.; Gratton, Y.; Marchese, C.; Poulin, M. Contrasting interannual changes in phytoplankton productivity and community structure in the coastal Canadian Arctic Ocean: Variability in Arctic phytoplankton dynamics. *Limnol. Oceanogr.* **2017**, *62*, 2480–2497. [CrossRef]
59. Giovanni | NASA Global Precipitation Measurement Mission. Available online: https://gpm.nasa.gov/data/sources/giovanni (accessed on 20 September 2023).
60. Cauwet, G.; Gadel, F.; de Souza Sierra, M.M.; Donard, O.; Ewald, M. Contribution of the Rhône River to organic carbon inputs to the northwestern Mediterranean Sea. *Cont. Shelf Res.* **1990**, *10*, 1025–1037. [CrossRef]
61. Coplen, T.B. Guidelines and recommended terms for expression of stable-isotope-ratio and gas-ratio measurement results. *Rapid Commun. Mass Spectrom.* **2011**, *25*, 2538–2560. [CrossRef] [PubMed]
62. Walton, W.R. Techniques for recognition of living foraminifera. *Cushman Found. Foraminifer. Res. Contr.* **1952**, *3*, 56–60.
63. Murray, J.W.; Bowser, S.S. Mortality, protoplasm decay rate, and reliability of staining techniques to recognize 'living'foraminifera: A review. *J. Foraminifer. Res.* **2000**, *30*, 66–70. [CrossRef]
64. Schönfeld, J.; Alve, E.; Geslin, E.; Jorissen, F.; Korsun, S.; Spezzaferri, S. The FOBIMO (FOraminiferal BIo-MOnitoring) initiative—Towards a standardised protocol for soft-bottom benthic foraminiferal monitoring studies. *Mar. Micropaleontol.* **2012**, *94*, 1–13. [CrossRef]
65. Corliss, B.H.; Emerson, S. Distribution of Rose Bengal stained deep-sea benthic foraminifera from the Nova Scotian continental margin and Gulf of Maine. *Deep Sea Res. Part Oceanogr. Res. Pap.* **1990**, *37*, 381–400. [CrossRef]
66. Bernhard, J.M.; Ostermann, D.R.; Williams, D.S.; Blanks, J.K. Comparison of two methods to identify live benthic foraminifera: A test between Rose Bengal and CellTracker Green with implications for stable isotope paleoreconstructions. *Paleoceanography* **2006**, *21*, 4. [CrossRef]
67. Fontanier, C.; Jorissen, F.; Licari, L.; Alexandre, A.; Anschutz, P.; Carbonel, P. Live benthic foraminiferal faunas from the Bay of Biscay: Faunal density, composition, and microhabitats. *Deep Sea Res. Part Oceanogr. Res. Pap.* **2002**, *49*, 751–785. [CrossRef]
68. Phipps, M.; Jorissen, F.; Pusceddu, A.; Bianchelli, S.; De Stigter, H. Live benthic foraminiferal faunas along a bathymetrical transect (282-4987 M) on the Portuguese margin (ne Atlantic). *J. Foraminifer. Res.* **2012**, *42*, 66–81. [CrossRef]
69. Mei, Z.-P.; Legendre, L.; Gratton, Y.; Tremblay, J.; LeBlanc, B.; Klein, B.; Gosselin, M. Phytoplankton production in the North Water Polynya: Size-fractions and carbon fluxes, April to July 1998. *Mar. Ecol. Prog. Ser.* **2003**, *256*, 13–27. [CrossRef]
70. Hamel, D.; de Vernal, A.; Gosselin, M.; Hillaire-Marcel, C. Organic-walled microfossils and geochemical tracers: Sedimentary indicators of productivity changes in the North Water and northern Baffin Bay during the last centuries. *Deep Sea Res. Part II Top. Stud. Oceanogr.* **2002**, *49*, 5277–5295. [CrossRef]
71. Redfield, A.C.; Ketchum, B.H.; Richards, F.A. The influence of organisms on the composition of seawater. *Sea* **1963**, *2*, 26–77.
72. Kravitz, J.H. Textural and Mineralogical Characteristics of the Surficial Sediments of Kane Basin. *J. Sediment. Res.* **1976**, *46*, 710–725. [CrossRef]
73. Sackett, W.M. The depositional history and isotopic organic carbon composition of marine sediments. *Mar. Geol.* **1964**, *2*, 173–185. [CrossRef]
74. Jasper, J.P.; Hayes, J.M. A carbon isotope record of CO2 levels during the late Quaternary. *Nature* **1990**, *347*, 462–464. [CrossRef] [PubMed]
75. Rau, G.; Sweeney, R.; Kaplan, I. Plankton 13C: 12C ratio changes with latitude: Differences between northern and southern oceans. *Deep Sea Res. Part Oceanogr. Res. Pap.* **1982**, *29*, 1035–1039. [CrossRef]
76. Rau, G.; Takahashi, T.; Marais, D.D.; Repeta, D.; Martin, J. The relationship between δ13C of organic matter and [CO2(aq)] in ocean surface water: Data from a JGOFS site in the northeast Atlantic Ocean and a model. *Geochim. Cosmochim. Acta* **1992**, *56*, 1413–1419. [CrossRef]
77. Teeri, J.A.; Stowe, L.G. Climatic patterns and the distribution of C4 grasses. *Oecologia* **1976**, *23*, 1–12. [CrossRef] [PubMed]
78. Ehleringer, J.R. Photosynthesis and photorespiration: Biochemistry, physiology, and ecological implications. *HortScience* **1979**, *14*, 217–222. [CrossRef]
79. Naidu, A.S.; Cooper, L.W.; Finney, B.P.; Macdonald, R.W.; Alexander, C.; Semiletov, I.P. Organic carbon isotope ratios (δ 13 C) of Arctic Amerasian Continental shelf sediments. *Int. J. Earth Sci.* **2000**, *89*, 522–532. [CrossRef]
80. Pomerleau, C.; Winkler, G.; Sastri, A.R.; Nelson, R.J.; Vagle, S.; Lesage, V.; Ferguson, S.H. Spatial patterns in zooplankton communities across the eastern Canadian sub-Arctic and Arctic waters: Insights from stable carbon (13C) and nitrogen (15N) isotope ratios. *J. Plankton Res.* **2011**, *33*, 1779–1792. [CrossRef]

81. Hobson, K.A.; Welch, H.E. Determination of trophic relationships within a high Arctic marine food web using δ 13 C and δ 15 N analysis. *Mar. Ecol. Prog. Ser.* **1992**, *84*, 9–18. [CrossRef]
82. Hobson, K.A. Reconstructing Avian Diets Using Stable-Carbon and Nitrogen Isotope Analysis of Egg Components: Patterns of Isotopic Fractionation and Turnover. *Condor* **1995**, *97*, 752–762. [CrossRef]
83. Altabet, M.A.; Francois, R. Sedimentary nitrogen isotopic ratio as a recorder for surface ocean nitrate utilization. *Glob. Biogeochem. Cycles* **1994**, *8*, 103–116. [CrossRef]
84. Francois, R.; Altabet, M.A.; Burckle, L.H. Glacial to interglacial changes in surface nitrate utilization in the Indian Sector of the Southern Ocean as recorded by sediment $\delta^{15}$N. *Paleoceanogr.* **1992**, *7*, 589–606. [CrossRef]
85. Farrell, J.W.; Pedersen, T.F.; Calvert, S.E.; Nielsen, B. Glacialá¤-interglacial changes in nutrient utilization in the equatorial Pacific Ocean. *Nature* **1995**, *377*, 514–517. [CrossRef]
86. Fox, A.; Walker, B.D. Sources and Cycling of Particulate Organic Matter in Baffin Bay: A Multi-Isotope δ13C, δ15N, and Δ14C Approach. *Front. Mar. Sci.* **2022**, *9*, 846025. Available online: https://www.frontiersin.org/articles/10.3389/fmars.2022.846025 (accessed on 16 October 2023). [CrossRef]
87. Scott, D.B.; Vilks, G. Benthic foraminifera in the surface sediments of the deep-sea Arctic Ocean. *J. Foraminifer. Res.* **1991**, *21*, 20–38. [CrossRef]
88. Saini, J.; Stein, R.; Fahl, K.; Weiser, J.; Hebbeln, D.; Hillaire-Marcel, C.; de Vernal, A. Holocene variability in sea ice and primary productivity in the northeastern Baffin Bay. *arktos* **2020**, *6*, 55–73. [CrossRef]
89. Steinsund, P.I.; Hald, M. Recent calcium carbonate dissolution in the Barents Sea: Paleoceanographic applications. *Mar. Geol.* **1994**, *117*, 303–316. [CrossRef]
90. Cedhagen, T. Retention of chloroplasts and bathymetric distribution in the Sublittoral Foraminiferan *Nonionellina Labradorica*. *Ophelia* **1991**, *33*, 17–30. [CrossRef]
91. Corliss, B.H. Morphology and microhabitat preferences of benthic foraminifera from the northwest Atlantic Ocean. *Mar. Micropaleontol.* **1991**, *17*, 195–236. [CrossRef]
92. Polyak, L.; Mikhailov, V. Post-glacial environments of the southeastern Barents Sea: Foraminiferal evidence. *Geol. Soc. Lond. Spéc. Publ.* **1996**, *111*, 323–337. [CrossRef]
93. Borrelli, C.; Panieri, G.; Dahl, T.M.; Neufeld, K. Novel biomineralization strategy in calcareous foraminifera. *Sci. Rep.* **2018**, *8*, 10201. [CrossRef]
94. Hald, M.; Korsun, S. Distribution of modern benthic foraminifera from fjords of Svalbard, European Arctic. *J. Foraminifer. Res.* **1997**, *27*, 101–122. [CrossRef]
95. Jorissen, F.J.; de Stigter, H.C.; Widmark, J.G. A conceptual model explaining benthic foraminiferal microhabitats. *Mar. Micropaleontol.* **1995**, *26*, 3–15. [CrossRef]
96. Van der Zwaan, G.; Duijnstee, I.; Dulk, M.D.; Ernst, S.; Jannink, N.; Kouwenhoven, T. Benthic foraminifers: Proxies or problems?: A review of paleocological concepts. *Earth-Sci. Rev.* **1999**, *46*, 213–236. [CrossRef]
97. Wollenburg, J.E.; Mackensen, A. Living benthic foraminifers from the central Arctic Ocean: Faunal composition, standing stock and diversity. *Mar. Micropaleontol.* **1998**, *34*, 153–185. [CrossRef]
98. Wollenburg, J.E.; Mackensen, A. On the vertical distribution of living (rose Bengal stained) benthic foraminifers in the arctic ocean. *J. Foraminifer. Res.* **1998**, *28*, 268–285. [CrossRef]
99. Odate, T.; Hirawake, T.; Kudoh, S.; Klein, B.; LeBlanc, B.; Fukuchi, M. Temporal and spatial patterns in the surface-water biomass of phytoplankton in the North Water. *Deep Sea Res. Part II Top. Stud. Oceanogr.* **2002**, *49*, 4947–4958. [CrossRef]
100. Burgers, T.M.; Miller, L.A.; Thomas, H.; Else, B.G.T.; Gosselin, M.; Papakyriakou, T. Surface Water $p$ $CO_2$ Variations and Sea-Air $CO_2$ Fluxes During Summer in the Eastern Canadian Arctic. *J. Geophys. Res. Ocean.* **2017**, *122*, 9663–9678. [CrossRef]
101. Jennings, A.E. Modern foraminiferal faunas of the southwestern to northern Iceland shelf: Oceanographic and environmental controls. *J. Foraminifer. Res.* **2004**, *34*, 180–207. [CrossRef]
102. Rytter, F.; Knudsen, K.L.; Seidenkrantz, M.-S.; Eiríksson, J. Modern distribution of benthic foraminifera on the north Icelandic shelf and slope. *J. Foraminifer. Res.* **2002**, *32*, 217–244. [CrossRef]
103. Corliss, B.H. Microhabitats of benthic foraminifera within deep-sea sediments. *Nature* **1985**, *314*, 435–438. [CrossRef]
104. Hald, M.; Steinsund, P.I. Distribution of surface sediment benthic Foraminifera in the southwestern Barents Sea. *J. Foraminifer. Res.* **1992**, *22*, 347–362. [CrossRef]
105. Polyak, L.; Korsun, S.; Febo, L.A.; Stanovoy, V.; Khusid, T.; Hald, M.; Paulsen, B.E.; Lubinski, D.J. Benthic foraminiferal assemblages from the southern Kara sea, a river-influenced arctic marine environment. *J. Foraminifer. Res.* **2002**, *32*, 252–273. [CrossRef]